

Bradley University

Lithium Ion Medium Power Battery Design

Final Report

By:

Jeremy Karrick
Charles Lau

Advisors:

Dr. Brian D. Huggins
Mr. Steve Gutschlag
Mr. Christopher Mattus

5/13/2010

Abstract

The objective of this project was to design and implement a Lithium Ion battery for medium power applications. Detailed measurements of charging and discharging behavior of cells and various cell configurations were made at various C rates. The data was used to facilitate design of the battery pack as well as the battery management system which includes cell balancing. A prototype passive cell balancing system was designed, built, and tested. In consideration of various battery models and experimental data, recommendations for the design of a medium power battery pack with cell management are presented.

Table of Contents

- I. Introduction.....3
- II. Project Goals3
- III. Functional Description and Block Diagram.....3
- IV. Functional Requirements and Performance Specifications.....4
- V. Battery Design
 - A. Structure.....5
 - B. Cell Balancing
 - 1. *SOC (State of Charge)*.....7
 - 2. *Need for Cell Balancing*.....7
 - 3. *Effects of Cell Balancing*.....8
- VI. Battery Implementation & Experimental Results
 - A. Battery Configuration and Capacity measurements.....13
 - B. Cell Balancing System Design
 - 1. *Hardware*.....20
 - 2. *Software*.....24
 - 3. *Experimental Results and Analysis*25
- VII. Recommendations for Future Work.....28
- IX. Standards.....28
- X. Bibliography.....29
- Appendix A30

I. Introduction

The popularity of low carbon footprint products is growing rapidly in a world of rapidly depleting fossil fuels. Such products need the capability of storing energy obtained from renewable energy sources such as wind turbines and photovoltaics. The most rapidly growing solution to this problem is the use of Lithium Ion technology, due to its high energy density and the predicted increase in availability with decreasing cost. Although Lithium Ion batteries can be currently found in many products from cell phones to electric vehicles, there is a surprisingly limited supply of Lithium Ion batteries that are available for medium power applications. Since the availability is limited but the demand seems to be increasing, it is the goal of this project to meet this growing demand via the design and implementation of a medium power battery module.

II. Project Goals

- Develop effective cell configuration and interconnections to yield compact medium power battery with appropriate capacity
- Make detailed recordings of cell behavior in various configurations while charging and discharging
- Incorporate a battery management subsystem to:
 - Accurately monitor state of cells during charging and discharging
 - Output data, in various formats, on state of cells
 - Balance the cells to maximize capacity
- Make recommendations for design of **an** effective medium power battery pack with cell management
- Ensure overall design is in compliance with industry standards

III. Functional Description & Block Diagram

The block diagram for the battery module is shown in Fig. 1 and consists of the battery pack made from individual cells, the cell monitoring electronics, and the switching circuits. Battery cells are connected together in combinations of series and parallel to form a battery pack exhibiting medium power characteristics with maximum efficiency. The battery cell configuration will be determined through experimentation and observation of cell behavior in these different configurations to determine the most efficient layout. As shown, the inputs to the battery module are user inputs and the outputs are cell parameters. Also, the battery will absorb or deliver power depending on whether it is being charged or discharged.

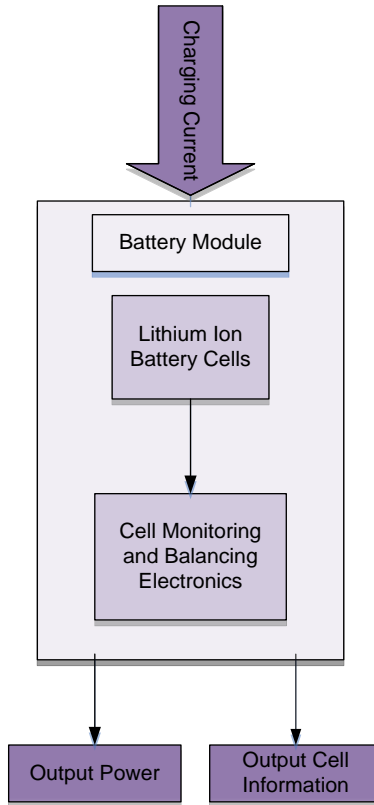


Figure 1

IV. Functional Requirements & Performance Specifications

The system will be designed under the following preliminary Performance specifications and requirements:

Physical

The combined total weight of the module shall be ≤ 13.6 Kg

The battery module shall measure $\approx 50 \times 50 \times 25$ cm.

The battery module shall meet functional specifications over a temperature range from $-20^{\circ}\text{C} \sim 60^{\circ}\text{C}$ in ambient air.

Electrical [Battery pack]

The battery pack shall have a nominal capacity ≈ 60 Ah.

The battery pack shall supply 1000W at a nominal voltage ≈ 24 V for one hour.

The battery pack shall have a current discharge limit of 60A continuous discharge.

The battery module shall retain functional specifications over ≥ 1000 charge/discharge cycles.

The battery module shall maintain compatibility with applicable commercial Lithium Ion chargers.

The battery module shall have protection circuit to ensure that the batteries individual cells cannot reach a temperature exceeding 94°C or can not be charged to a voltage exceeding 3.6V or decrease below 2.8V.

Electronics [based on test mode operation]

The battery module shall include monitoring circuitry accurate to 3%

The monitoring circuitry shall record the voltage and current flow throughout the battery pack.

The monitoring circuitry shall upload performance data collected from the multiple sensors to a PC through a USB interface

V. Battery Design

A. Structure

The battery structure is a large part of battery design. Learning the behavior of battery cells and choosing the best cell configuration will optimize the performance of the battery pack in any given application. The most basic behavior of battery cells when combined is that cells connected in parallel add capacity overall and cells that are connected in series add voltage to the pack. However, battery design is more complicated than these simple rules since cell behavior is impacted by the connections between cells and connections to the load. Lithium ion batteries are among the most difficult chemistries to work with because of their unique behaviors in these different combinations. In series, these types of cells have a tendency to imbalance during charge or discharge. Parallel battery connections also exhibit unique behaviors that are not expected or intuitive.

In general, batteries in parallel balance to each other, shown by the way they naturally equalize voltage. This behavior can be seen below in figure 2, where two batteries that exhibit an open circuit terminal voltage that differs by roughly 40mV, representing a small difference in state of charge. The batteries are connected in parallel with an ammeter put between the cells to monitor current flow between them. It can be seen that the battery cell with the higher state of charge will drain current into the battery cell with a lower state of charge until they equalize.

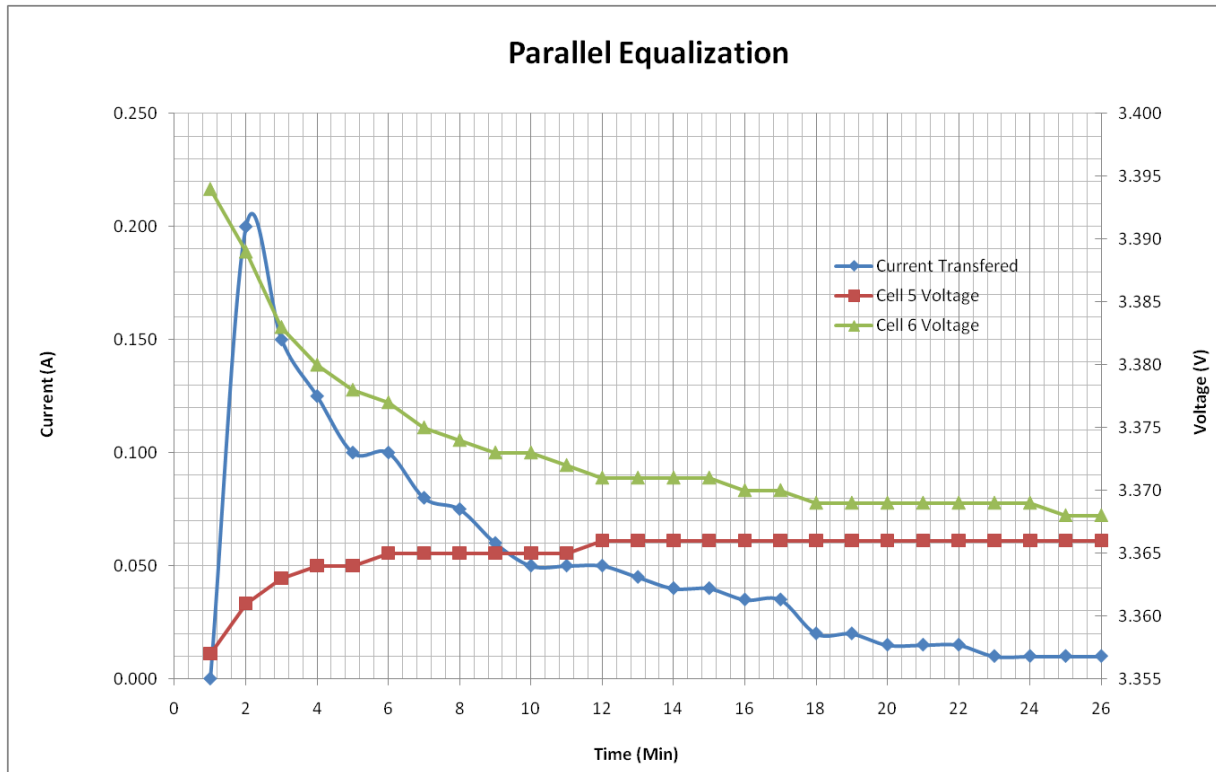


Figure 2

However, behavior exhibited by batteries in parallel can also be somewhat counter-intuitive. By the physical makeup of a battery, they have a very small internal resistance. Ours was measured to be roughly $12\text{m}\Omega^*$. Because this resistance is so small, other resistances in the circuit start to affect the current flow when they would usually be negligible. Specifically all connections in the circuit as well as wires have small resistances that begin to affect how these batteries behave. It was discovered that to avoid many problems the batteries in parallel must be connected to the load in a symmetrical fashion as shown in figure 3 as opposed to a nonsymmetrical connection as shown in figure 4. When the batteries are connected in a nonsymmetrical configuration to the load, the current from the cell physically further from the load discharges almost an order of magnitude less current than the cell physically closer to the load. This type of behavior limits the capacity of the configuration, since the closest cell will fully discharge before the second cell, thereby leaving unused capacity in the furthest cell. This will be covered more in the experimental results and analysis section.

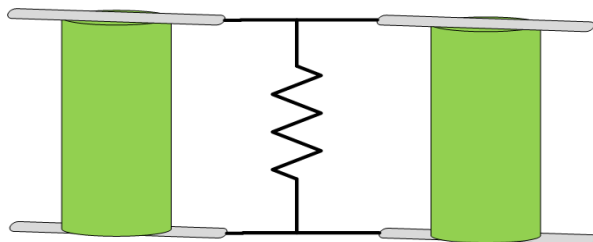


Figure 3

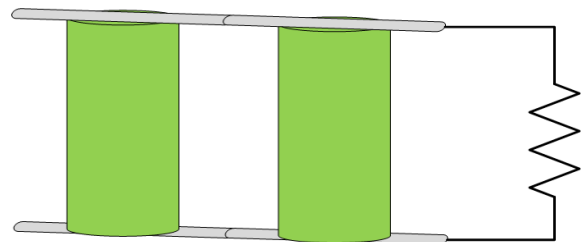
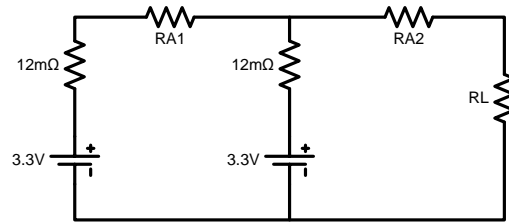


Figure 4

*this measurement could vary, since the precise measurements needed to calculate this required a greater accuracy than that of the fluke used.



Circuit 1

Above circuit 1 shows the thevenin's equivalent circuit for two batteries in parallel with an unsymmetrical load. Upon analyzing the circuit it can be determined that the current moving across RA2 as compared to RA1 will be much larger. This is expected, however, upon closer inspection, it is determined that most of the current passing through RA2 is from the second battery (closest to RL). This is exactly what happens when the load is connected unsymmetrically to two cells in parallel.

B. Cell Balancing

1. SOC (State of Charge)

SOC is defined as $SOC = \text{Remaining Capacity} / \text{Rated Capacity}$ where capacity is measured in amp hours.

2. Need for Cell Balancing

The motivation for research and development of a lithium ion cell balancing system is to maximize the total capacity of the battery. When cells in a battery have different SOC values, the charge and discharge cycles will decrease. The charging process is stopped when one cell reaches 100% SOC and the discharge process is stopped when one cell reaches 0% SOC. When the cells are unbalanced, some cells will not reach 100% SOC; therefore, the capacity of the battery will decrease. A small imbalance in a battery will have accumulative an effect on the capacity of the battery over time. The idea of cell balancing is to bring all the cells to the same SOC while the cells are charging, discharging, or at rest.

Lithium ion cells exhibit SOC defects due to tiny imperfections in the internal structures of the cells. This occurs from a change in the chemical composition due to age and exposure to extreme temperatures.

Initial SOC unbalance occurs in the event of a poor quality process during manufacturing. This is the uncommon defect and a cell with this kind of defect can not be corrected 100%.

Varying SOC pertains to the rate at which particular cells can be charged (charge acceptance rate) or discharged. This also includes the rate of energy loss a cell experiences while being stored, which is referred as the self discharge rate. All cells have a self discharge rate. When the self discharge rate is relatively higher than other cells, then it is considered a SOC defect. Figure 5 gives a graphical representation of two cells that are unbalanced cells due to a high self discharge rate. The first plot shows the accumulative effect of a SOC defect. One cell does not charge to 100%, therefore the

discharge cycle is shortened. The second plot shows the cells when they are balanced. The charge of one cell is slowed down in order to provide enough time for the defective cell to charge up to 100%, hence increasing the capacity of the battery. In this case, cell balancing is necessary for all charge cycles during the life of the battery. [Cell Balancing Maximizes the Capacity of Multi-cell Li-Ion Battery Packs by Carlos Martinez, Intersil, Inc.; <http://www.analogzone.com/pwrt0207.pdf>]

3. Effects of Cell Balancing

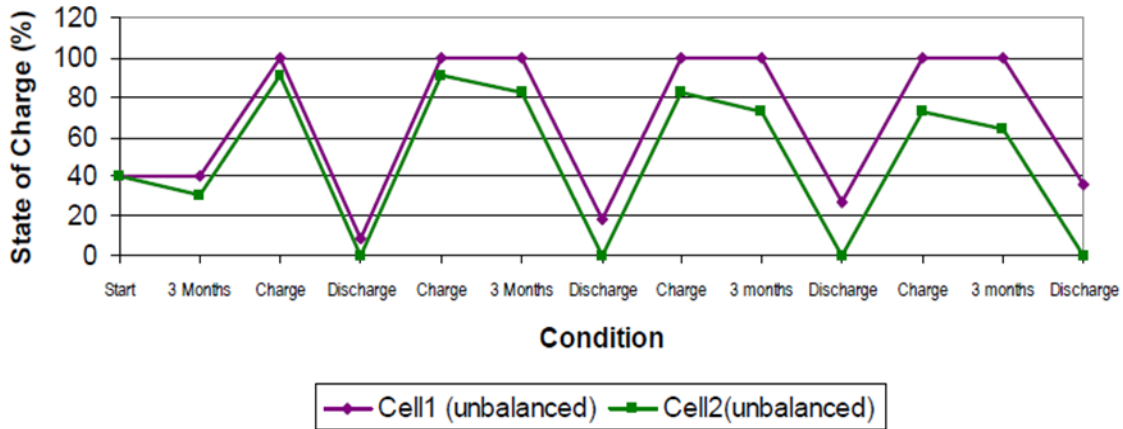


Fig. 1: Cell Capacity With No Cell Balancing

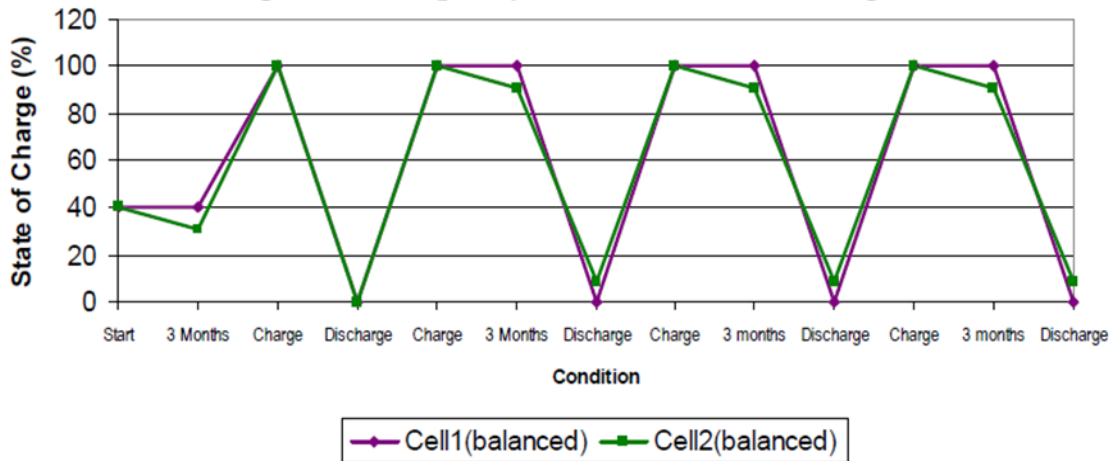


Fig. 2: Cell Capacity With Cell Balancing

Figure 5 (Carlos Martinez)

a. Variables That Effect the SOC

- Voltage
- Current
- Temperature

- Internal Resistance

The OCV (open-circuit voltage) is the primary indicator of the SOC; however, the relationship between the SOC and the OCV is non-linear and also depends on many other variables. Techniques used for charge estimation algorithms include fuzzy logic, Kalman filtering, and neural Networks. Graphical representations of SOC vs. OCV relationships are expressed in figures 7 and 8. [Electropaedia, State of Charge Determination, <http://www.mpoweruk.com/soc.htm#lookup>]

Capacity reduction under varying temperatures and discharge rates are shown in figure 6. The reduction of capacity implies that the SOC will decrease faster during the discharge cycle.

Capacity reduction at different temperatures and discharge rates

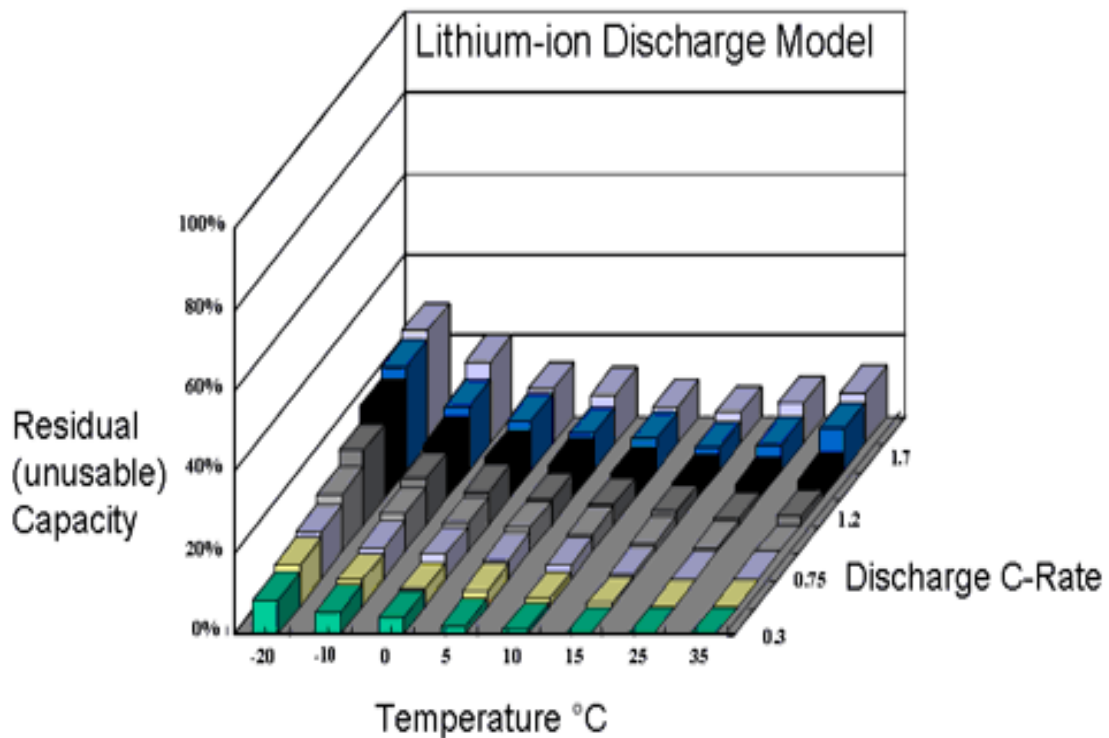


Figure 6 (Woodbank, 2005)

A high discharge rate will decrease the OCV while discharging. Charging and discharge currents in real life applications are rarely kept at a constant value, therefore current should be considered an input for a cell balancing system. Figure 7 shows discharge characteristics with different discharge rates.

Discharge Characteristics, 25 deg C

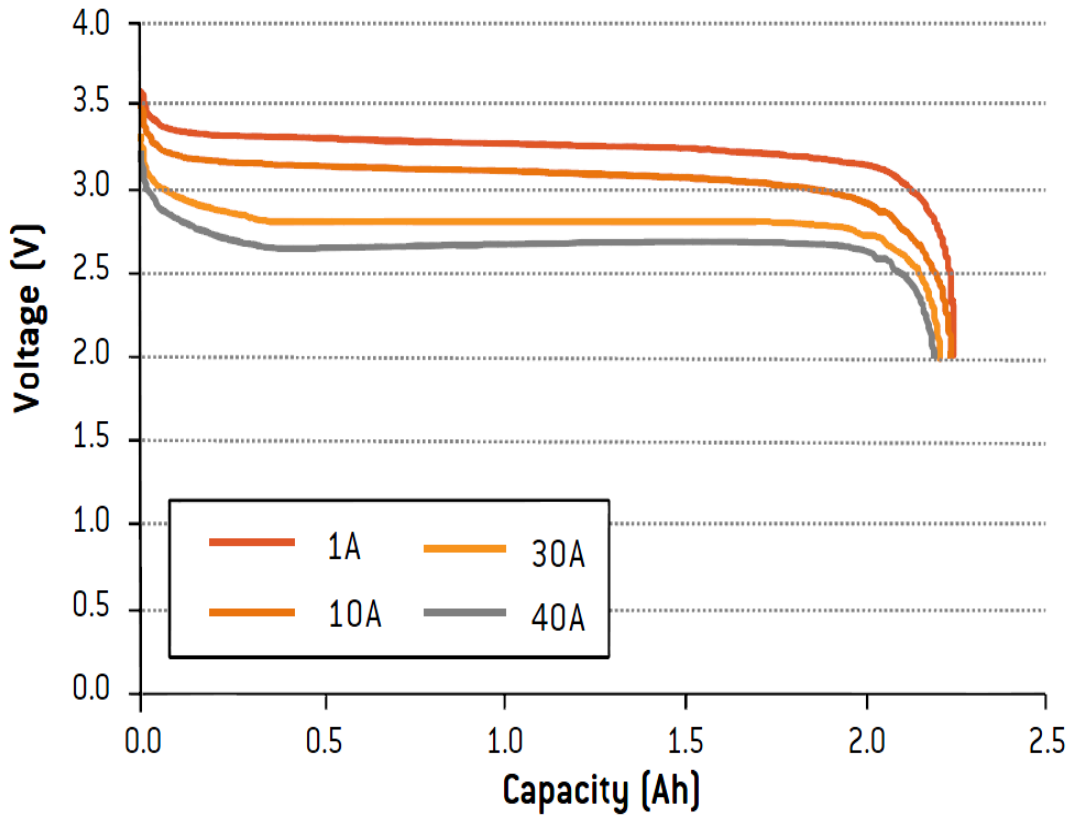


Figure 7

Extreme temperatures will cause the SOC to decrease faster. A high temperature will cause the OCV to increase and a low temperature will cause OCV to decrease. Temperature should be considered as an input for a cell balancing system in a battery is exposed to large temperature differences. Figure 8 shows low temperature discharge performance for lithium-Ion cells.

The internal resistance of a cell will have an effect on its charge and discharge acceptance. Impedance measurements of a cell may be beneficial to calculate the SOC and to determine a cell model.

Low Temperature Discharge Performance

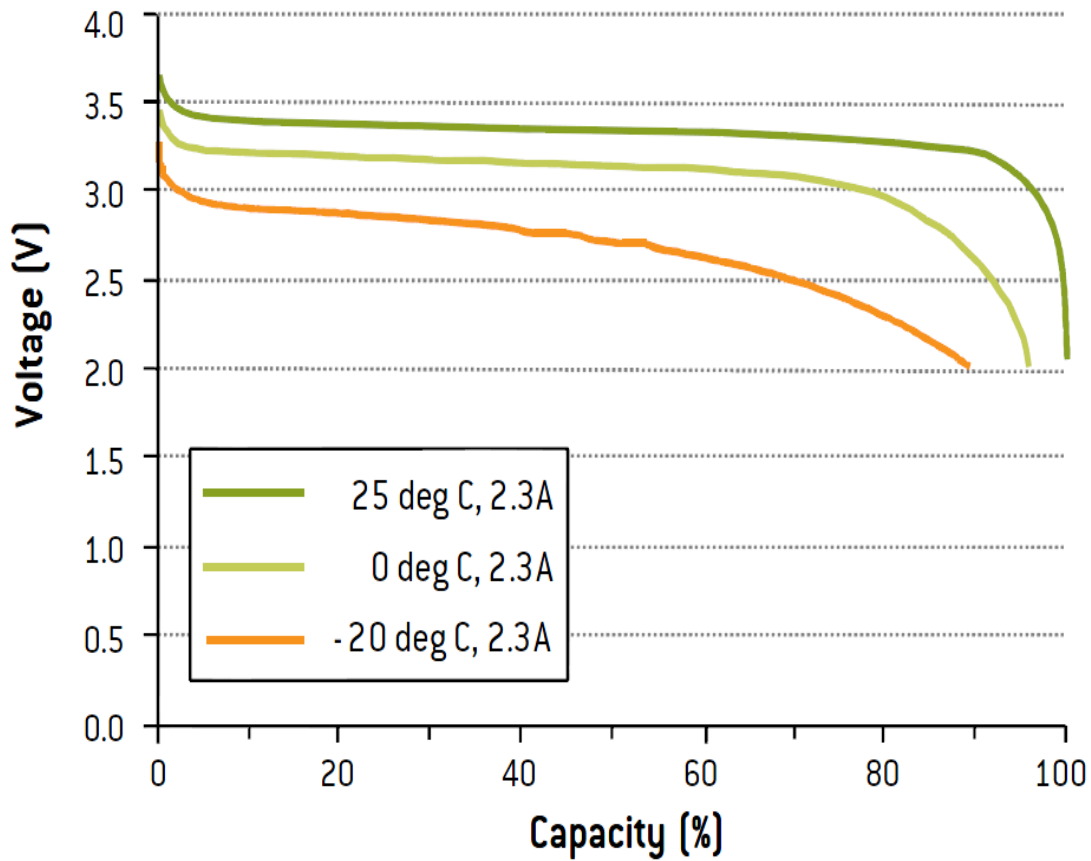


Figure 8
From A-123 Datasheet

b. Techniques for Cell Balancing

Passive (Dissipation) Approach:

The passive approach in cell balancing implies shunting current through a resistor in parallel to the cell with the highest SOC in order to dissipate energy from that cell. This will allow the cell with the lowest SOC to further increase its SOC. The passive approach is a common method, even though it wastes energy. Due to the heat produced by this approach, it is more efficient for low powered applications. See figure 9 for the basic schematic of the passive balancing approach.

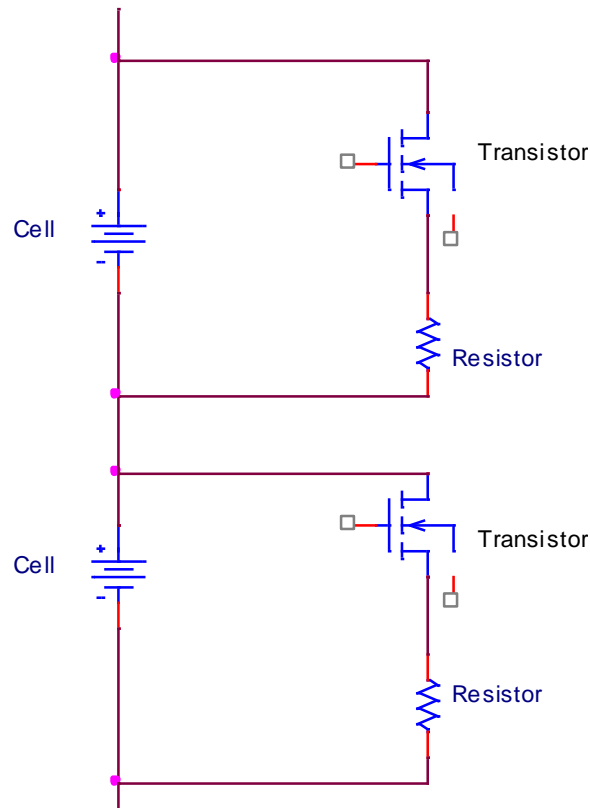


Figure 9

Active (Redistribution) Balancing Approach:

The Active balancing approach implies transferring energy from the cell with the highest SOC to the cell with the lowest SOC using a storage element such as an inductor or a capacitor. This method requires more components than the passive balancing approach, therefore it is a more expensive design. The cost of this design will out way the efficiency concerning low powered applications; however, the active approach is more efficient for high powered applications.

Two popular active approach designs include using a capacitor and using a transformer. In the case of the capacitor, or flying capacitor method, a capacitor is place in parallel to one cell at a time. It will be charged with one cell. Then a switch will cause the capacitor to be in parallel to another cell and transfer its energy to that cell. The transformer design can be implemented in three ways. In the first design, the primary side of the transformer is in parallel to the stack, while the secondary side is in parallel to one individual cell at a time. This is a transfer of energy from the stack to an individual cell. The second design is the opposite of the first, meaning energy is transferred from one cell to the stack. The third design is set up like the flying capacitor; meaning the energy is transferred from cell to cell.

VI. Battery Implementation & Experimental Results

A. Battery Configuration and Capacity measurements

A great deal of time was spent in experimentation with different combinations of batteries to observe behavior of the cells and what effects these combinations would have on a battery pack. The first step to learning about the characteristics of cells in different combinations would be to observe how they behave alone. To assist with the study of the behavior of battery cells a commercial battery charger was purchased from Bantam Tek. This charger, the BC6-10, is capable of charging up to 6 Lithium Ion cells in series and can charge with a maximum constant current of 10A. The charger was ideal for this application because it included balancing capabilities (for early experimentation while this projects balancing system was still under development). The charger also included some software as well as a USB interface and was capable of recording real-time information into charts as seen in figure 10 below. The capability to record data in this manor was instrumental in the study of the behavior of lithium ion battery cells.

Figure 10 shows a charge cycle of a single Lithium Ion battery cell. Characteristics of this charge cycle that should be noted are that constant current is supplied until the cell voltage reaches 3.6V; at this point the voltage is held at 3.6 and a top-off current is supplied and slowly drops off until about .05A suggested by the data sheet. This top-off current will be greater or less depending on the C-rate the battery is charged at. At lower C-rates it is likely that the battery will not require any top-off current, conversely at higher C-rates, the battery will need much more current than shown below.

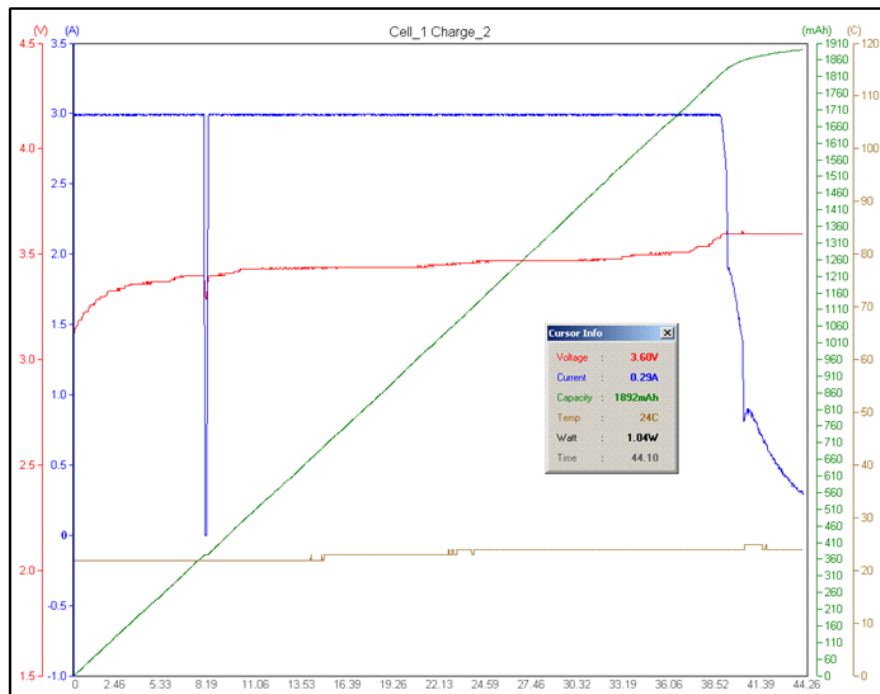


Figure 10

It is also observable here that the capacity put into the cell was only 1932mAh which is under the rated capacity of the battery by almost 400mAh. The reason for this was simply the discharge that can be seen below in figure 11. Here we notice that the discharge was cut off when the battery cell was only

2.99V instead of the recommended cut-off terminal voltage of 2.0V. This was probably a minor bug or 1 time occurrence in the charger. But the important thing to see is that the battery only discharged 1939mAh which is very close to the capacity that was put into the cell during the charge.

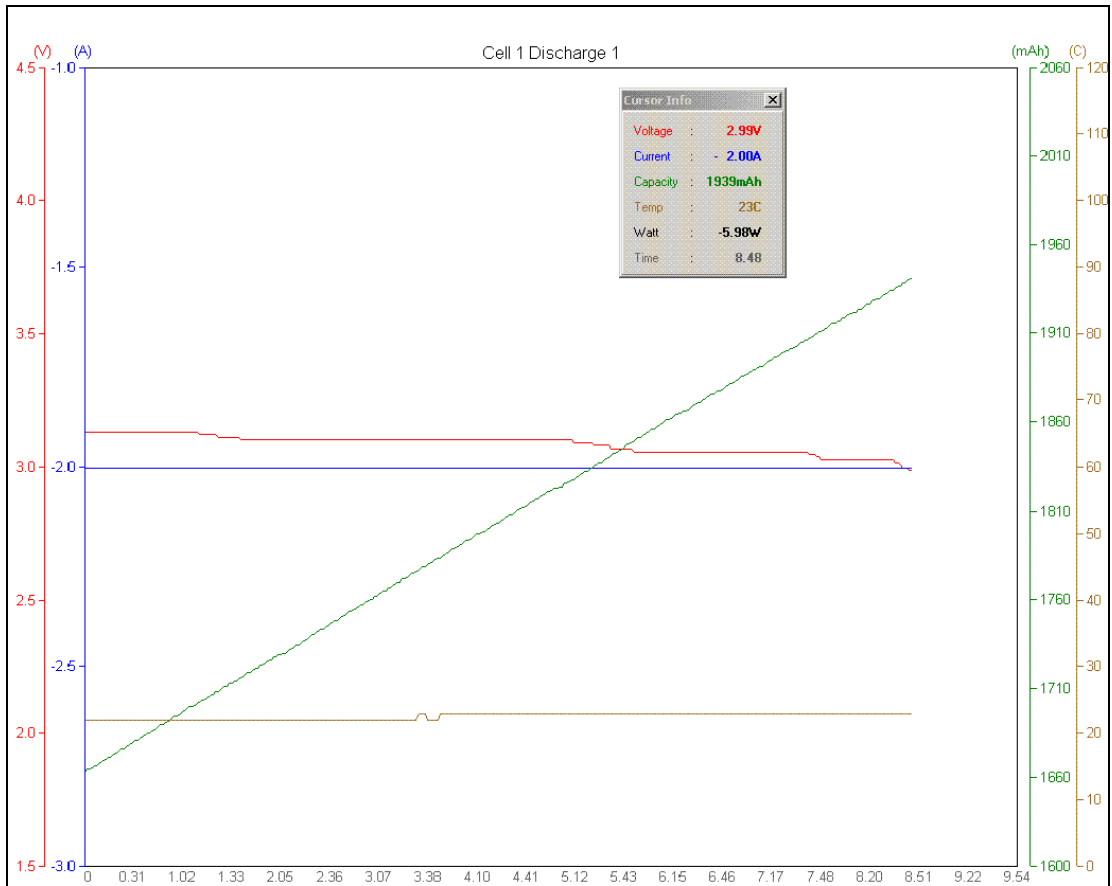


Figure 11

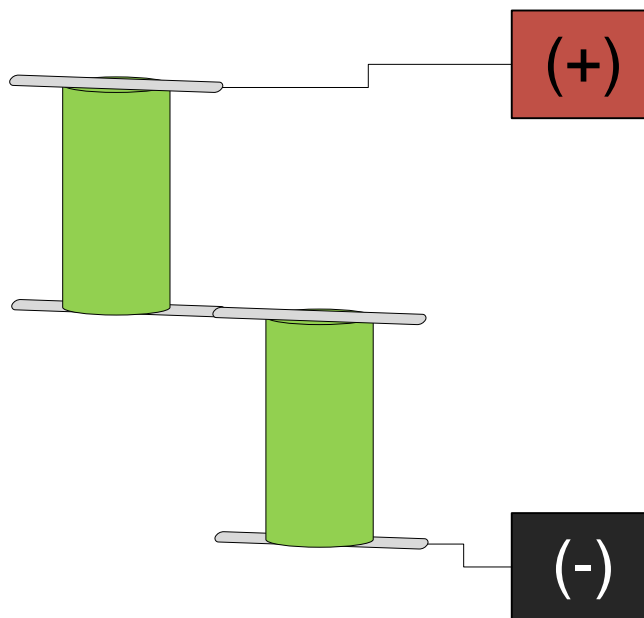


Figure 12

Batteries in series, as stated before, have a tendency to unbalance during a charge or discharge causing a loss in overall capacity of the battery pack. This was witnessed during experimentation even over small periods of single cycles, and was estimated to get much worse over time if left uncorrected. The physical way that the batteries were connected in series can be seen above in Figure 12. In figure 13, it can be seen that after a simple charge the voltage differences between the cells can have a large effect on the efficiency of a charge and on the capacity in general. Although the cells seen in Figure 13 below, where only charged from the initial 50% SOC (the state of charge they where shipped at), there is still a small but noticeable lack of capacity, since they would be expected to show at least 1150mAh. It can also be seen that there is several places where it seems there is an inconsistency with the cells. On the voltage curve of the graph, after the batteries reach 7.2V total, they would have ideally been kept at that constant voltage for the top-off portion of the charge, however it clearly fluctuates and falls slightly from this ideal voltage. Also, while observing the top-off current, it can be seen that there are oscillations present in the amount of current flowing to the cells. Finally, by looking at the box in the bottom right of the figure, which shows the voltages of the individual cells, it can be seen that they are at least 20mV apart from each other, which is the cause of the anomalies shown here.

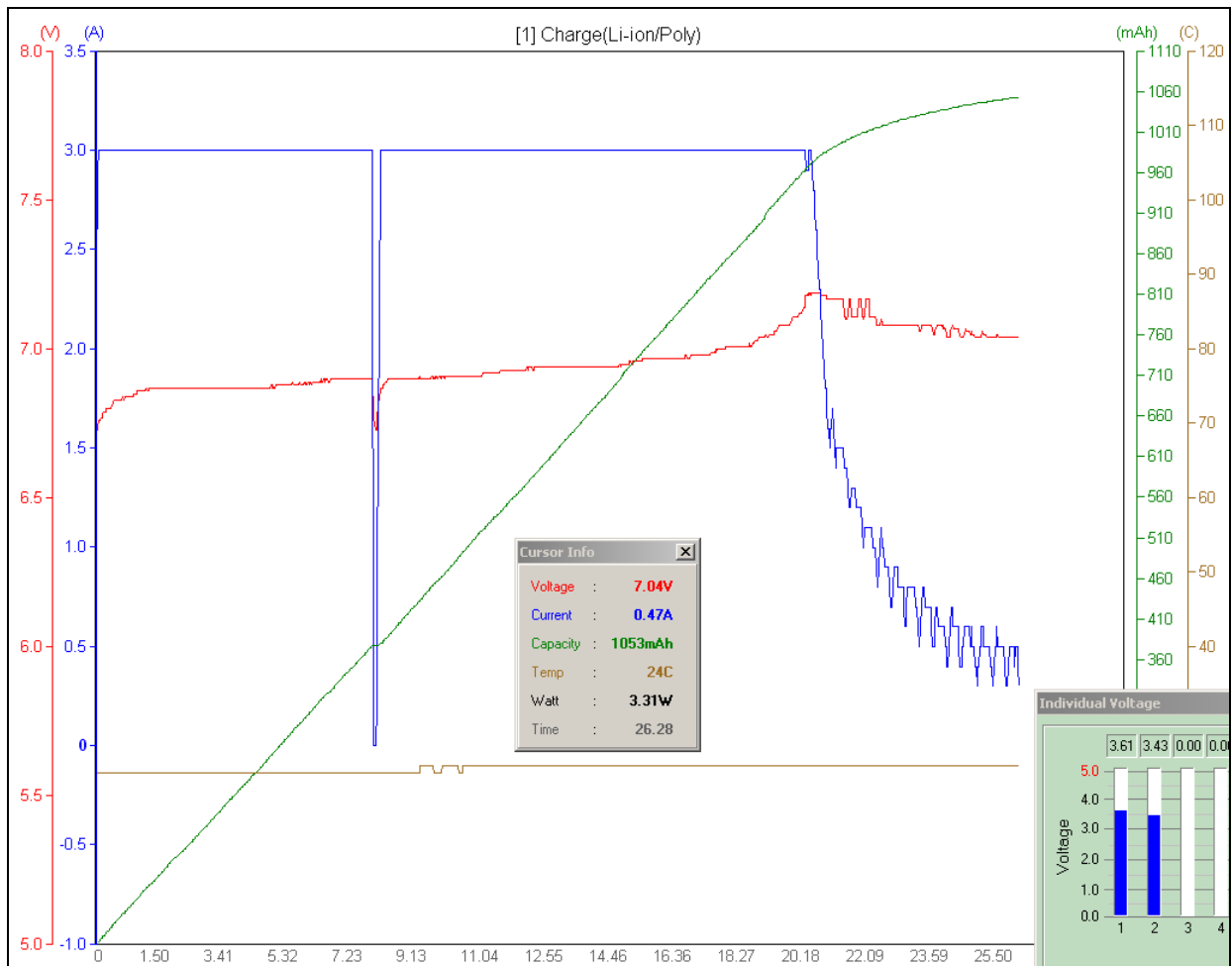


Figure 13

Experimentation with batteries in parallel was performed with the batteries connected as seen in a previous section in figure 3. It was stated earlier that when batteries connected in parallel must be connected in a symmetric configuration. This can be further verified by the data seen below in figure 14 and figure 15; where figure 14 is the graph of a battery discharged into a load asymmetrically and figure 15 shows a battery discharged into a load connected symmetrically. The most notable part of the graphs is the difference in capacity measured. In the asymmetrical case the capacity is lessened by almost a quarter as compared to when the load is connected symmetrically.

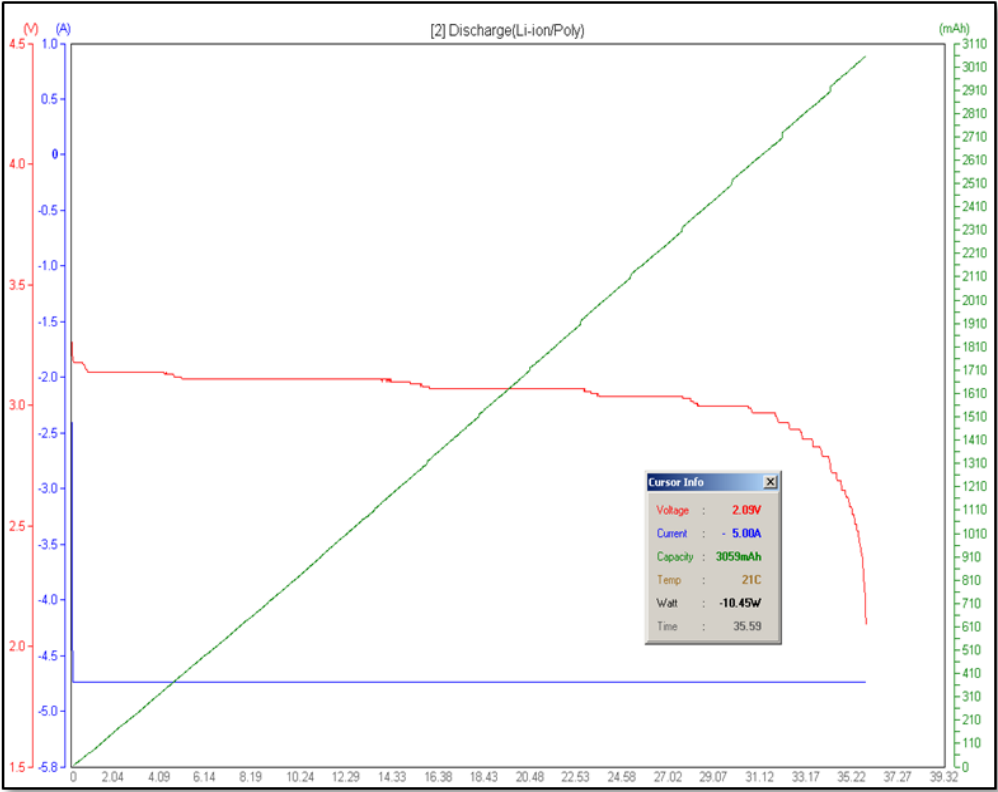


Figure 14

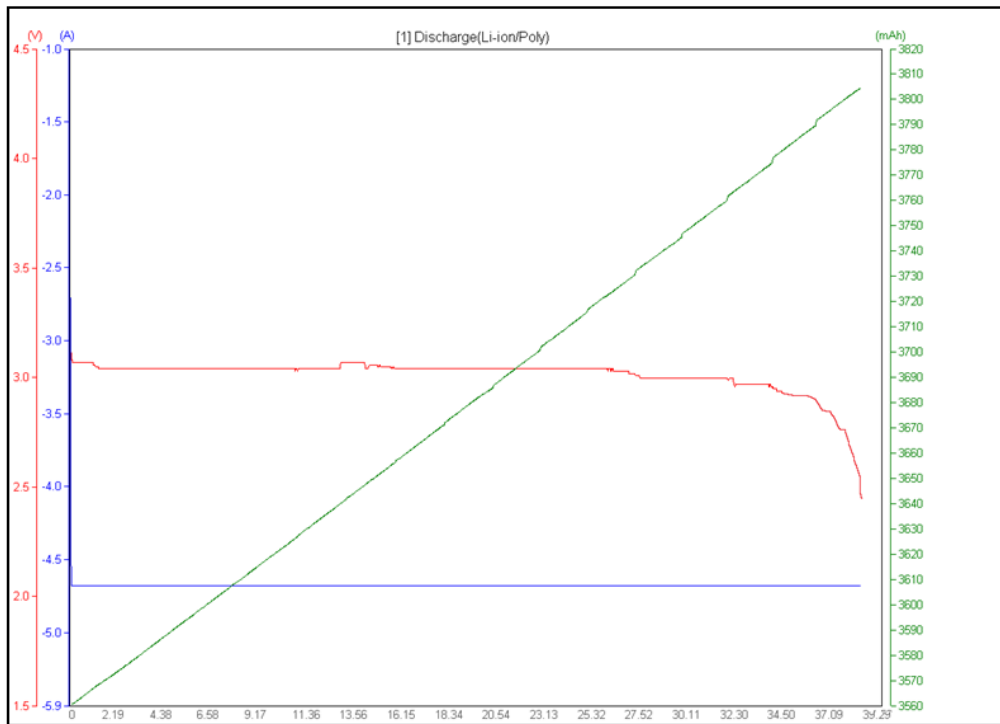


Figure 15

A battery pack combines batteries in both series and parallel, which means that the battery pack exhibits traits from both types of combinations, making it difficult to work with. Three configurations were proposed for the general battery pack design. The first method for combining cells into a battery pack, seen in figure 16(a), shows that the batteries would be configured in two stacks of cells in series, which are then combined in parallel. This method resulted in a loss of capacity of about 25%. Data showing a charge cycle can be seen below in figure 17. The loss in capacity has to do with balancing. The pack in this configuration has two stacks of batteries in series and unfortunately this creates an issue with using any standard balancing system, since the balancing systems are designed to compare battery voltages of cells up the stack, having two stacks creates a lot of unnecessary complications when attempting to balance. In most cases this results in only one stack being balanced, which can lead to unbalancing in the second stack, thus resulting in any one of the cells in the second stack reaching the minimum voltage of the cell first, and thereby cutting off the entire pack even though many other cells may still have capacity left.

The next proposed configuration, shown in Figure 16(b) shows that the cells would be connected in parallel and then these parallel pairs would be connected in series. This configuration exhibits the same problems as discussed in the section about parallel batteries and symmetrical load connections. Since the load is not connected symmetrically between the batteries, the same loss of capacity is visible here and can be seen in Figure 18. This configuration also shows a loss of almost 50% capacity.

The Final configuration, shown in figure 16(c), through experimentation, was established to be the best method of creating a battery pack. This configuration utilizes all the concepts learned earlier about the behavior of cells when connected together to form battery packs. This method requires the least amount of separate monitoring sensors, the least complicated balancing design, and the best usable capacity of all three configurations. The balancing can be done by simply monitoring the voltages at the

center of the parallel connection of each pair of cells, and the natural behavior of cells in parallel and in symmetry will keep the voltages of the pairs in parallel very close, meaning no further balancing for the pairs is required.

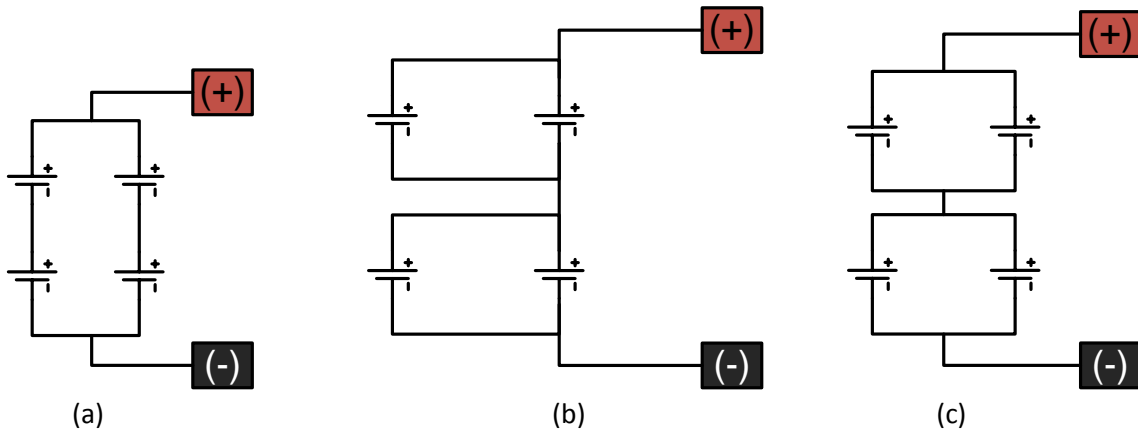


Figure 16

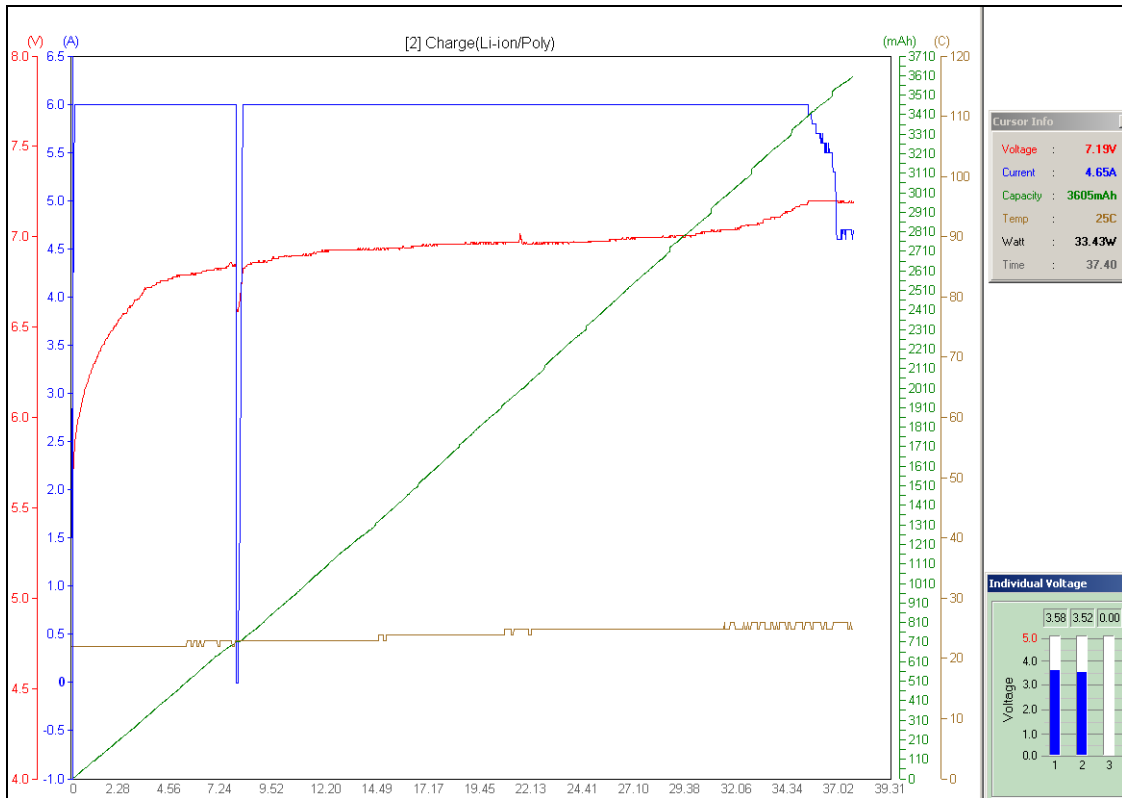


Figure 17

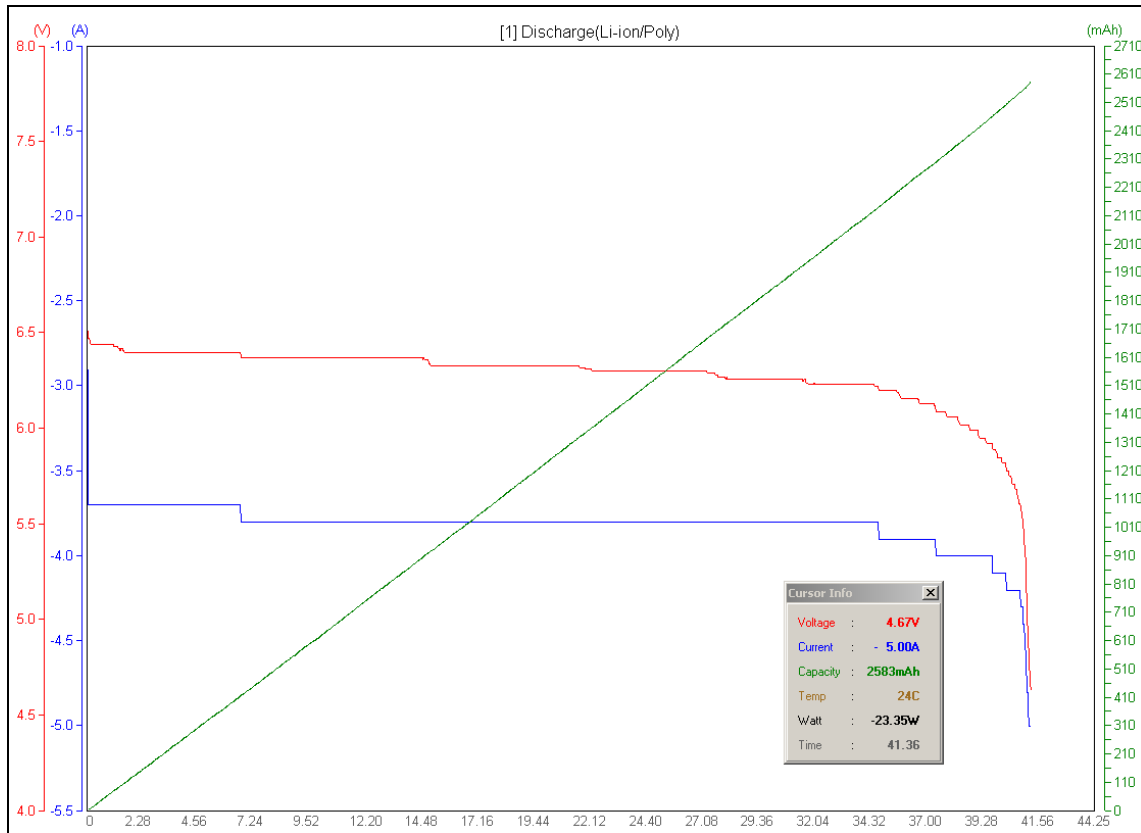


Figure 18

B. Cell Balancing System Design

1. Hardware

The passive balancing approach was selected with the basic structure shown in figure 19. Current was kept at a constant level during charge and discharge. Temperature changes during experimental discharge and charge cycles were relatively small. From experimental data, it was observed that the voltage decreased the whole time through a discharge and increased the whole time during a charge. Furthermore, the difference in magnitude of the low slope voltage curve was 250mV. Due to these controlled conditions, terminal voltage was used as the only indicator of a difference of the SOC of individual cells. See Figure 10 to see the experimental data while charging. The accuracy of the cell balancing system is designed for 20mV, which is the lowest precision that the 8051 microcontroller's A/D precision can be set to. Figure 19 Shows the overview block diagram of the Passive Cell Balancing System for three cells.

Overview Block Diagram of the Passive Cell Balancing System

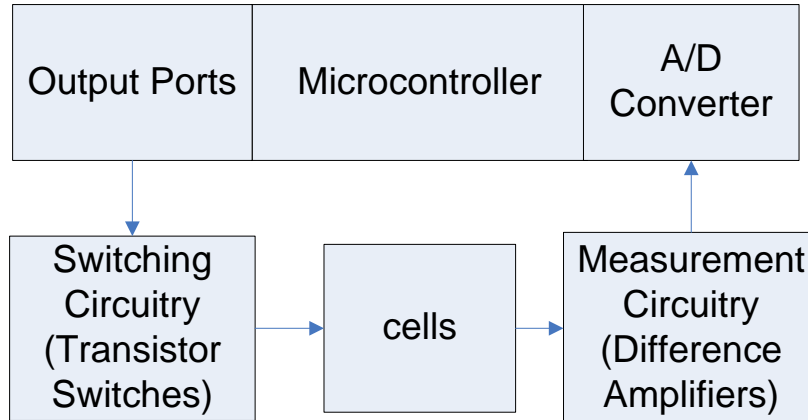


Figure 19

Measurement Circuit

Voltage followers were used to prevent current from flowing to the microcontroller. Consideration of CMRR is required in the design of the measurement circuitry. The relative accuracy of the output of the difference operational amplifiers are to be within 20mV. If the error of accuracy of the measurement circuit were greater than 20mV, then the microcontroller would not be able to make an appropriate decision concerning the switching circuitry. The measurement schematic for the three cell balancing system is shown in figure 20.

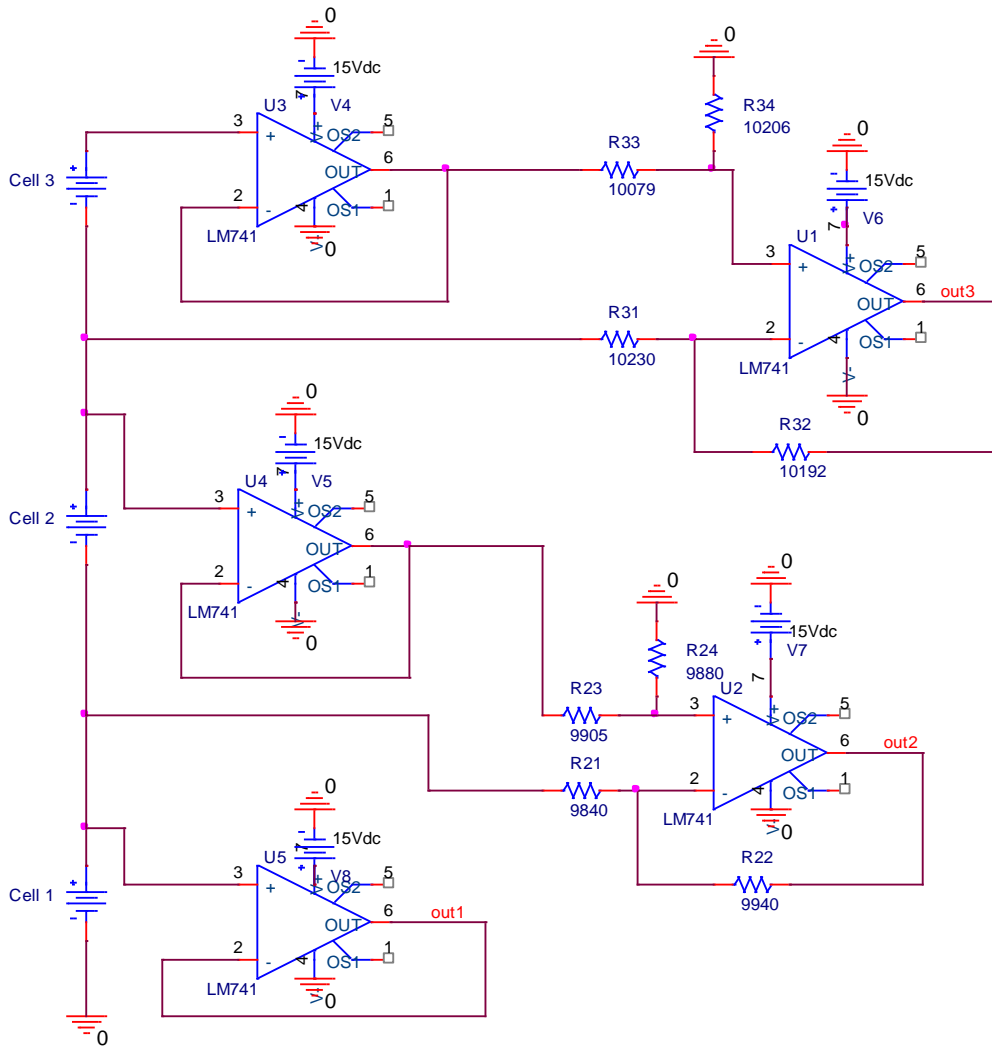


Figure 20

Circuit Equations for Analysis of Measurement Circuitry

- 1) $V_o = A_d * V_{id} + A_{cm} * V_{icm}$
- 2) $A_d = R_2 / R_1$
- 3) $V_{id} = V_2 - V_1$
- 4) $V_{icm} = \frac{1}{2} * (V_2 + V_1)$
- 5) $A_{cm} = [R_4 / (R_4 + R_3)] * \{1 - [(R_2 * R_3) / (R_1 * R_4)]\}$

Design concerns pertaining to the measurement circuit include the consideration of the common mode gain and the differential gain. Five percent standard resistors were used in the design which made it difficult to attain an accuracy of 20mV or less. The strategy used to determine the resistor values is to first choose R1 and R2. These resistors will determine the differential gain of the amplifier. R3 should be

as close to R1 as possible. The common mode gain will need to offset the differential gain. This becomes a greater issue as the voltage measurements become greater. After selecting R1, R2, and R3, equation #1 will allow for calculation of an ideal common mode gain. Using equation #5, the common mode gain equation, an idea value for R4 can be found.

Switching Circuitry

The switching schematic for the three cell balancing system is shown in figure 21.

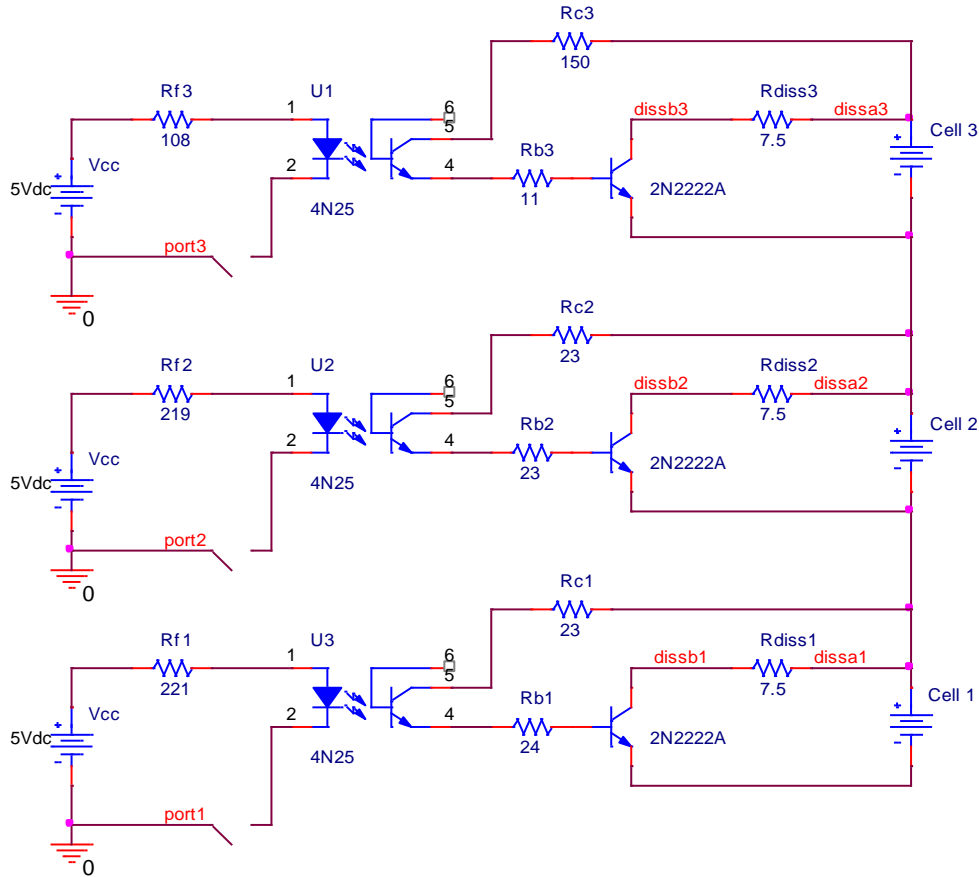


Figure 21

Design concerns involving the switching circuitry included the current through the dissipation resistor, current through the input diode of the optocoupler, saturation of the transistors, and the maximum ratings of the components in the circuit. The current through the dissipation resistors are specified to be 400mA.

Determination of the shunting current was considered analytically and experimentally. Important factors concerning the shunting current include the power dissipation or temperature produced by the shunting resistor and the time desired to balance the cells. An analytical approach to determine the shunting current is as follows.

$$I_{diss} = (\text{total \% difference of SOC}) * (\text{cell capacity[Ah]}) / (\text{time desired to balance the cells [h]})$$

[Cell Balancing Maximizes the Capacity of Multi-cell Li-Ion Battery Packs by Carlos Martinez, Intersil, Inc.; <http://www.analogzone.com/pwrt0207.pdf>]

For example, if cell 1 is at 100% SOC, cell 2 is at 85% SOC, and cell 3 is at 95% SOC, then the total SOC difference is 20%. The time desired is arbitrarily set to 2 hours. Therefore the dissipation current is as follows for this example.

$$I_{diss} = (0.2) * (2.3Ah) / (2h) = 230mA$$

Table 22 shows the experimental results with different dissipation resistor values.

Table 22 Experimental Results

Date of Experiment	4/20/2010	4/20/2010*	4/21/2010	5/10/2010
Dissipation Resistor	32.1 ohms	7.5 ohms	10 ohms	7.5 ohms
Dissipation Current	105mA	445mA	151mA	373mA
Rate of Voltage Drop	0.9 mV/min	9.3 mV/min	1.1mV/min	2mV/min
Power Dissipation	0.36w	1.49w	0.23w	1.04w

*This experiment was done without a transistor. A cell was placed in parallel with a 7.5 ohm resistor.

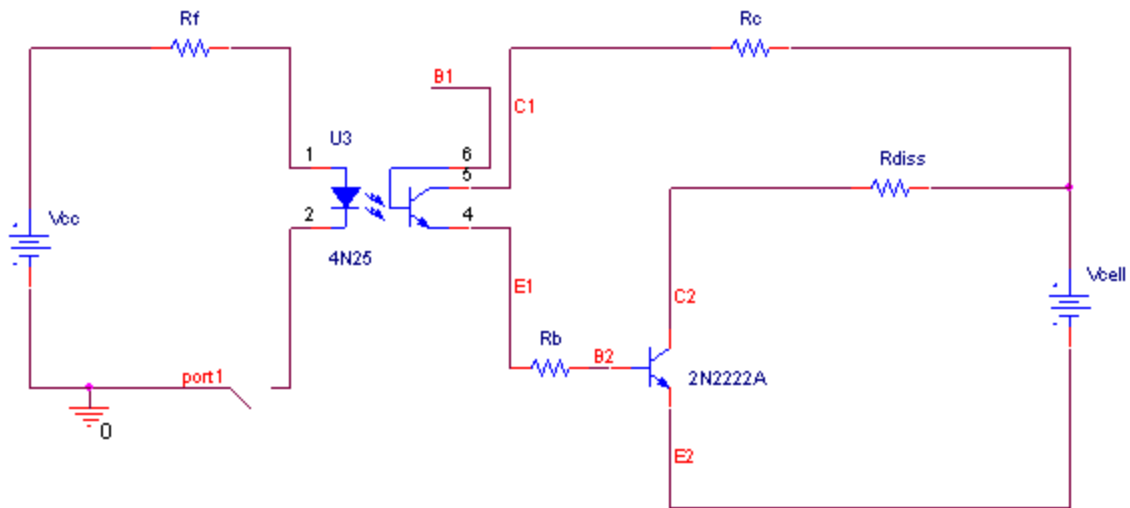


Figure 23 (Switching Circuitry Schematic for analysis)

Design Equations for Saturation

- 1) $V_{ce} = 0.2v$
- 2) $V_{be} = 0.7v$
- 3) $V_{cb} = -0.5v$
- 4) $V_c + V_{bc1} + V_{be1} + V_b - V_{cb2} - V_{diss} = 0$
- 5) $V_{diss} + V_{cb2} + V_{be2} - V_{cell} = 0$
- 6) $V = I * R$

7) $V_f = 3.7$

8) $I_c / I_b = \text{Beta}$

Using figure 23 as a reference, resistors R_c and R_b need to be chosen appropriately to force the transistors to be in saturation of the switching to occur and to optimize the dissipation current. It will be found that the maximum V_{diss} value is $V_{cell} - 0.2$. This will provide a good estimate of the shunting current (I_{diss}) or the shunting resistor (R_{diss}); which ever one is being solved for. The optocoupler datasheet shows a relationship between I_f and I_c . Equation #4 will allow for a calculation of V_c and V_b , hence R_b and R_c can be chosen. Saturation of the optocoupler transistor can be checked by measuring V_{ce} , V_{be} , and V_{cb} . Saturation of the 2N2222 transistor can be check the same way or by using equation #8.

2. Software

The cell balancing system includes the use of a 8051 microcontroller. The voltage from the output of the difference operational amplifiers to ground is detected by the microcontroller's A/D channels. The A/D precision is set at 20mV. The A/D conversion is performed every second. The binary values are sent to the "Compare Module" to determine which cell, if any, requires dissipation of energy. If there is a cell which requires the dissipation of energy, then the appropriate output port is set to zero, allowing the appropriate transistor switch to turn on. See figure 24.

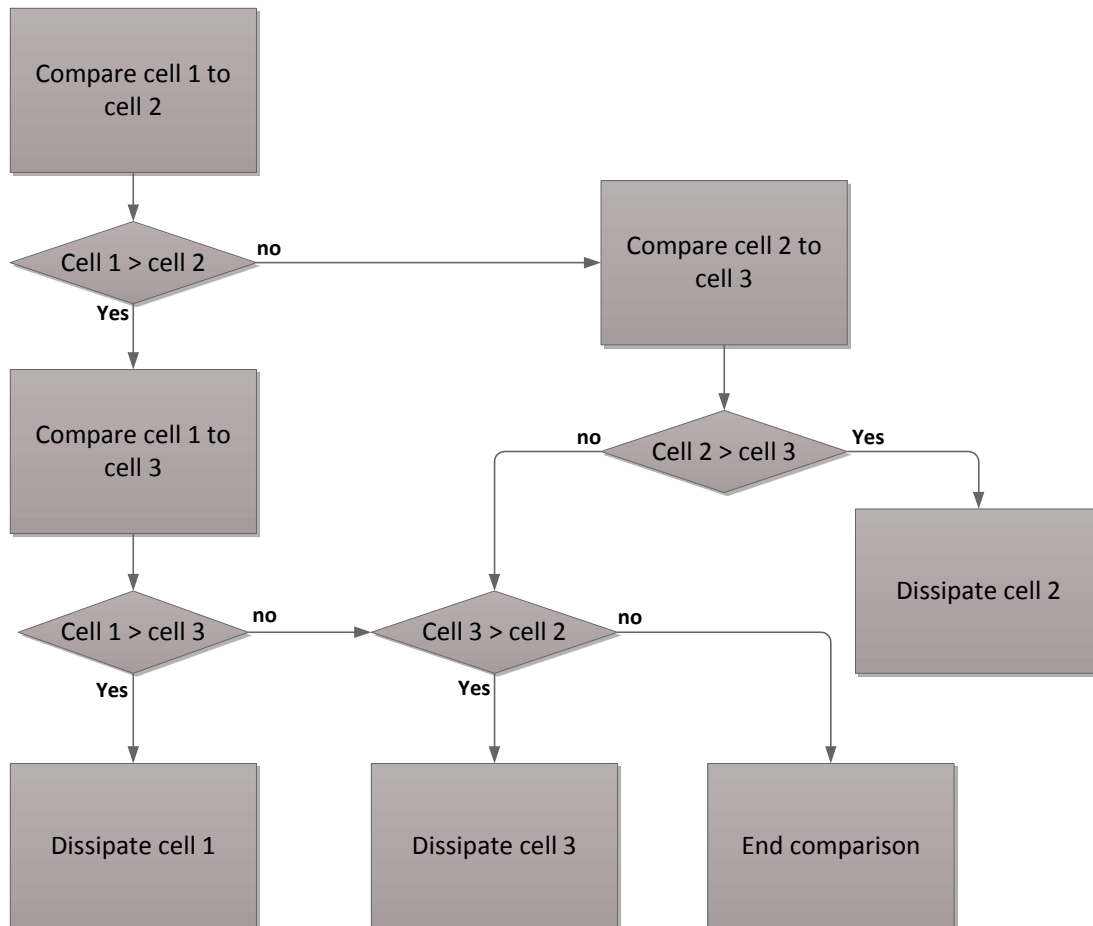


Figure 24

3. Experimental Results and Analysis

Further calculations were performed on the difference operational amplifiers in the measurement circuitry after the demonstration. It was found analytically that if R4 on the second difference operational amplifier should be changed to 10073 ohms to produce an error of less than 1 mV. Results of the measurement circuit and the analytical errors are shown in table 25. Note that the first cell is not measured by a difference operational amplifier.

Table 25 (Measurement Circuit Results)

<u>Cell Voltage</u>	<u>Output Voltage</u>	<u>Actual Error</u>	<u>Analytical Error</u>
V cell 3 = 3.383	V out 3 = 3.382	Error = -1mV	Error = 54mV
V cell 2 = 3.370	V out 2 = 3.365	Error = -5mV	Error = 2mV
V cell 1 = 3.269	V out 1 = 3.263	Error = -6mV	

Switching Circuit Results

The switching circuitry was functional but not optimized. See table 26. The transistors in the optocoupler were not in saturation; however, all the 2N2222 transistors were. The switching circuit results are for $V_{cell} = 3.294v$. The desired dissipation current was 400mA.

Table 26

	Switch 1	Switch 2	Switch 3
Vf (v)	3.812	3.828	3.819
Vce1 (v)	0.156	1.881	1.035
Vbe1 (v)	0.7	0.738	0.6839
Vbc1 (v)	0.547	-1.146	-0.459
Vce2 (v)	0.25	1.283	0.341
Vbe2 (v)	0.868	1.834	0.814
Vbc2 (v)	0.63	0.551	0.485
Vdiss (v)	2.9	2.919	2.853
Vc (v)	0.197	0.266	1.184
Vb (v)	0.199	0.265	0.079
Idiss (mA)	387	389	380
Pdiss (w)	1.121	1.136	1.085

Demonstration Results

Three parallel combinations of cells were placed in series. See figure 27. Each parallel combination consisted of two cells. Measurements were observed at each parallel combination. Each parallel combination was connected to the switching and measurement circuitry. Initially, the first combination (V1) was measured to be 30mV lower than the other two (V2 and V3). When the cell balancing system was activated, switch 2 turned on. This was indicated by measuring the voltage across the input resistor to the optocoupler. The voltage across the dissipation resistor was measured to be 2.8V. About five minutes after initiation, V2 decreased to within 10 mV of V1. Switch 2 turned off for one second and then turned on again. Switch 2 repeated to turn off for one second about every twenty seconds. The voltage across the dissipation resistor was measured to be 2.8v, therefore the dissipation current was 373 mA.

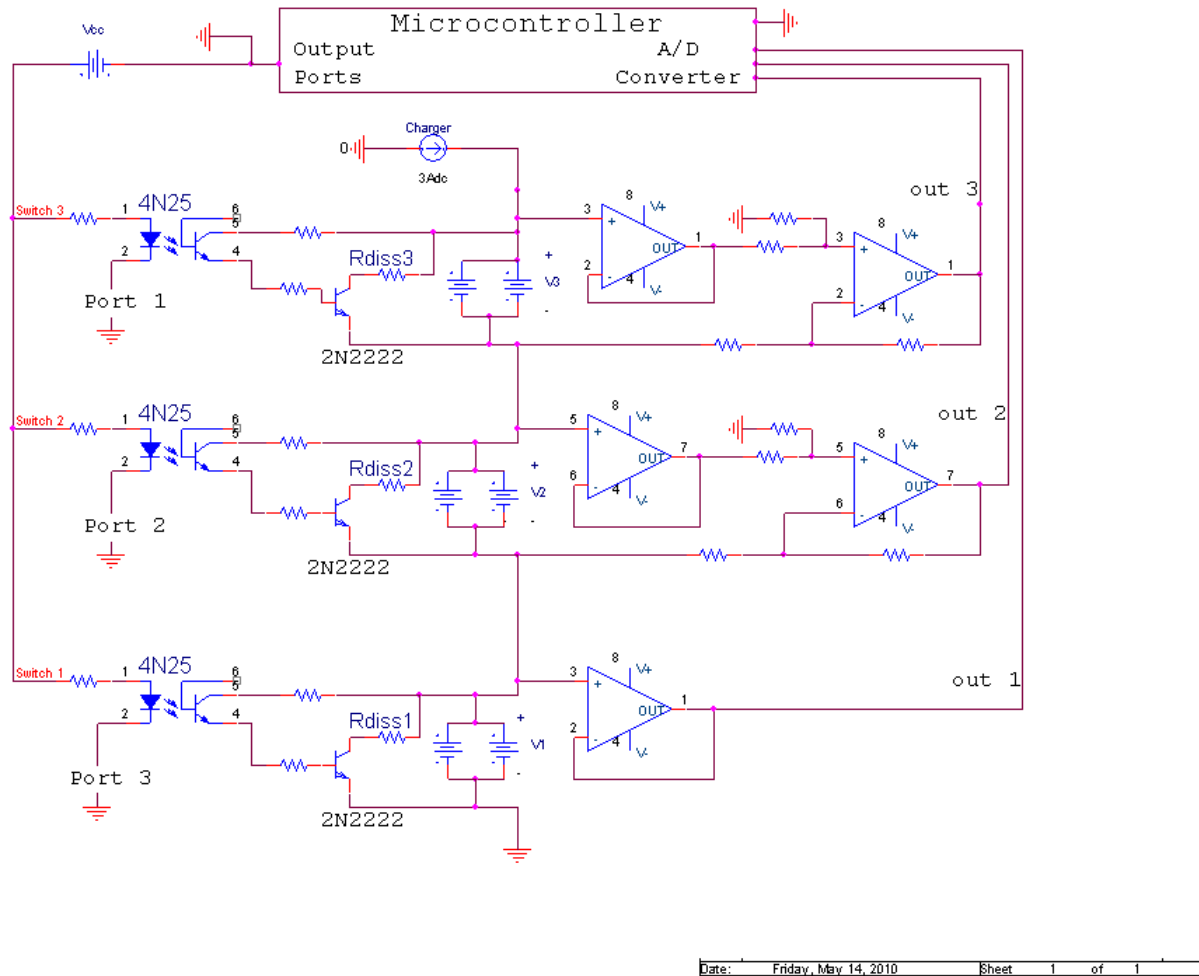


Figure 27

Explanation of Demonstration Results

Switch 2 will turn off when V2 is within the 20mV range that V1 presides in. However, when the switch is turned off, the current through cell 2 increases. It was previously discovered during charge experiments that when a charge is initiated, the voltage of a cell will experience a sudden rise in voltage. When switch 2 was on, the current through cell 2 is theoretically 2.6A. When Switch 2 is turned off, the current through cell 2 is increased by 400mA. The voltage rise due to the 400mA increase is not as high as the voltage rise from the 3A when turning the charger on, yet the 400mA increase is enough to cause V2 to rise above the 20mV range that V1 presides in. In short, V2 is bouncing above the voltage range of V1. When V2 drops low enough, switch 2 will turn off. Then V2 rises due to the rise in current causing switch 2 to turn on again.

A solution to this problem is to leave switch 2 on longer. Perhaps switch 2 should stay on until V2 reaches the 20mV range below V1; however, this would require the voltage rise to be less than 20mV.

VII. Recommendations for Future Work

This project has several areas in which a future project could expand and improve upon the current progress. The first objective of any future work planned for this project should be to acquire larger capacity cells. The cells should be the capacity that is required due to known complications with the behavior of cells in parallel mentioned earlier. If no cells of adequate size are available combining two cells in parallel would be a relatively simple task and would be a secondary option.

Another major area of improvement from a standpoint of safety would be the current interrupts and general switching circuitry to be designed and put in place between cell interconnects. While for a majority of our testing it was generally assumed that through the low usage, the cells would stay intact and not experience any faulty behavior from a bad cell, however through more abuse it is possible for a cell to go bad and become a short circuit which could pose a real danger as a fire hazard and electrocution hazard.

Since the ultimate goal of the project is to reach medium power applications, it would be an extreme advantage to implement an active balancing system. The levels of current that this battery would be discharging, a passive balancing system would need to dissipate far too much heat in order to effectively balance the cells and would therefore no longer be efficient. An active balancing system would be better suited for this design.

Also for future work, the battery pack as a whole would be much easier to handle if all of the cells and their monitoring equipment were interfaced through a single microprocessor. By keeping all processes to a single processor the system would be easier to handle and manipulate, as well as be more efficient since all switching commands and information would be handled by the same thing.

IX. Standards

Safety is a primary concern when dealing with lithium ion batteries, since there is possibility of fire or explosions if handled or used incorrectly. Underwriters Laboratories and SAE International both have standards pertaining to the safe use of Lithium Ion Batteries. UL has two specific standards that apply to this project: Standard 1642 – Covers requirements for safety in operation and testing pertaining to Lithium ion rechargeable multi-cell batteries, and standard 2054 – Covers requirements for safety in operation and testing pertaining to household and commercial batteries in regards to preventing fires and explosions. SAE International has one applicable standard: AS5679 - Minimum performance standard for Li-Ion rechargeable single and multiple cell batteries. Currently, no publication of this standard is available to the public. J1797 – Recommended practice for packaging of electric vehicle battery modules. This SAE Recommended Practice provides for common battery designs through the description of dimensions, termination, retention, venting system, and other features required in an electric vehicle application. The document does not provide for performance standards. As of 2008, a standard for the characterization of lithium battery technologies in terms of performance, service life and safety attributes is still under development by IEEE with no word on when these will be complete or available to the public.

X. Bibliography

Buchmann, Isidor. Learning the Basics About Batteries. 2003. 10 2009 <<http://batteryuniversity.com/>>.

"High Power Lithium Ion ANR26650M1A." 1 4 2009. a123 Systems. 10 2009
<http://a123systems.textdriven.com/product/pdf/1/ANR26650M1A_Datasheet_APRIL_2009.pdf>.

Multi-cell Li-Ion polymer Battery Charger with Fuel Gauge. 10 2009. 12 2009
<<https://secure.cypress.com/?id=1021&rtID=201&rID=23&cache=0>>.

Wen, Sihua. "Cell Balancing Buys Extra Run Time and Battery Life." 17 3 2009. Texas Instruments, Incorporated. 12 2009 <<http://focus.ti.com.cn/cn/lit/an/slyt322/slyt322.pdf>>.

Martinez, Carlos. "Cell Balancing Maximizes the Capacity of Multi-Cell Li-Ion Battery Packs." 2005. Analog Zone. 2009 <<http://www.analogzone.com/pwrt0207.pdf>>.

Stephen W. Moore, Peter J. Schneider. Copyright © 2001 Society of Automotive Engineers, Inc.

<http://www.mpoweruk.com/soc.htm>. Copyright © Woodbank Communications Ltd 2005

Appendix A – Cell Specifications from Datasheet

Cell Characteristics

Nominal Capacity - 2.3 Ah

Nominal Voltage - 3.3 V

Charging Parameters

Charge Current – 3.0 A

Charge Voltage -3.6 V

Cut-off Charge Current for CV - .05 A

Float charge voltage – 3.45 V

Max. Charge Voltage 3.8 V

Max Charge Current – 10 A

Discharging Parameters

Discharge cut-off voltage – 2.0 V

Max. continuous Discharge Current 60 A